GA–A24763

ELM-INDUCED PLASMA TRANSPORT IN THE DIII–D SOL

by
J.A. BOEDO, D.L. RUDAKOV, E.M. HOLLMANN, G.R. McKEE,
R.A. MOYER, K.H. BURRELL, T.E. EVANS, L. ZENG, A.W. LEONARD,
J.G. WATKINS, and W.P. WEST

JUNE 2004

DISCLAIMER

GA–A24763

ELM-INDUCED PLASMA TRANSPORT IN THE DIII–D SOL

by
J.A. BOEDO,* D.L. RUDAKOV,* E.M. HOLLMANN,* G.R. McKEE,†
R.A. MOYER,* K.H. BURRELL, T.E. EVANS, L. ZENG,‡ A.W. LEONARD,
J.G. WATKINS,Δ and W.P. WEST

This is a preprint of a paper to be presented at the 31st European Conf. on Plasma Physics and Controlled Fusion, London, United Kingdom, June 28 through July 2, 2004 and to be published in the *Proceedings.*

*University of California, San Diego, California
†University of Wiscosin, Madison, Wisconsin.
‡University of California, Los Angeles, California.
ΔSandia National Laboratories, Albuquerque, New Mexico.

Work supported by
the U.S. Department of Energy
under DE-FG02-04ER54758, DE-FG03-96ER54373, DE-FG03-01ER54615, DE-FC02-04ER54698, and DE-AC04-84AL85000

GENERAL ATOMICS PROJECT 30200
JUNE 2004

ELM-Induced Plasma Transport in the DIII–D SOL

J.A. Boedo[1], D.L. Rudakov[1], E.M. Hollmann[1], G.R. McKee[2], R.A. Moyer[1], K.H. Burrell[3], T.E. Evans[3], L. Zeng[4], A.W. Leonard[3], J.G. Watkins[5], and W.P. West[3]

[1]*MAE Department, UCSD, 5600 Gilman, La Jolla, CA 92093-0417, USA*
[2]*University of Wisconsin, Madison, University, Madison, WI, USA*
[3]*General Atomics, San Diego, CA, USA*
[4]*University of California, Los Angeles, CA, USA*
[5]*Sandia National Laboratories, Albuquerque, NM, USA*

I. Introduction

High performance tokamak discharges operate in H-mode with edge localized modes (ELMs) to combine high-energy confinement with adequate particle exhaust. However, the ELM instability also carries a considerable amount of particles and heat from the pedestal region into the SOL towards the divertor region and other plasma facing components (PFCs), possibly limiting their lifetime and causing the release of impurities into the plasma. According to accepted scalings, Type I ELMs potentially could exceed the ITER PFC damage threshold (40 to 50 MJ m^{-2} t^{-1}) by factors of 5 or more [1], resulting in a divertor lifetime of less than one full discharge. Therefore, it is important to invest a significant effort to study the ELM dynamics in the SOL in order to envision ways of controlling their interaction with the PFCs. A number of theoretical studies [2] of ELMs have emphasized that in the linear regime, the dominant modes, [3] referred to as coupled "peeling-ballooning" modes, are driven by both parallel current (J_{ped}) and the pressure gradient (p'_{ped}). These intermediate-n peeling-ballooning modes, whose linear phase can be calculated using the ELITE code [3], impose limits on the pedestal height, which are functions of the pedestal width, plasma shape, collisionality, safety factor and other equilibrium details. Preliminary nonlinear studies [4] suggest that during the ELM, filaments will grow in the pedestal region and travel across the separatrix into the scrape-off layer (SOL), carrying particles and heat with them. This paper provides information on ELM structure and propagation that can be used to improve the nascent non-linear ELM modeling work.

II. Experimental Setup

Experiments to characterize ELMs on the DIII–D tokamak [5] were carried out in H-mode discharges featuring Type I ELMs with plasma current I_p = 1.4 MA, toroidal field of B_T = 1.7 T at the axis, R = 1.7 m and neutral beam heating power of up to 4.5 MW. Lower single-null divertor geometry with ion Grad-B drift toward the lower divertor was used. The density was increased in a sequence of discharges, from $\langle n_e \rangle / n_G = 0.40$ to 0.8. (n_G is the Greenwald density limit). The principal measurements presented were made by the fast radiometer array [6] (DISRAD2), a fast scanning probe

[7], beam emission spectroscopy (BES) [8], reflectometry [9] and CER [10]. The fast scanning probe array features five tips that sense current I, saturation current, I_{sat}, and floating potential, Φ_f. A ≈250 kHz bandwidth T_e measurement [11] is used to resolve the temperature inside the ELMs. The BES system, configured as a 5×6 fiber array, was located at the edge of the plasma in the midplane to provide fast (1μs) 2-D imaging of the density. The DISRAD2 measures absolutely calibrated photon intensity along 30 poloidally separated view chords at a rate of 100 kHz and a photon energy response of 1 eV to 5 keV.

III. ELM Characterization and Dynamics

Two frames from BES taken at an arbitrary time near an ELM onset, t_0^{BES} and 16 μs later ($t_0^{\mathrm{BES}}+16\mu$s) and shown in Fig. 1, show an ELM as a positive density perturbation appearing at the bottom of the frame and moving upward to the center. The data shown is the deviation from the average value and in the color scheme, white represents average (or background) density and red and blue represent positive and negative fluctuations respectively, black indicates saturation. The LCFS is indicated by a solid vertical line. The two main observations are that: 1) the ELM is poloidally and radially localized in the low field side (LFS) and, 2) it includes plasma ejections (indicated by a circle) produced near the separatrix that then move radially outward. Inversion of the DISRAD2 data measuring the integrated ELM radiation for various plasma regions as a function of time indicates that the radiation rises first on the outer SOL, indicating low field side ELM formation [12,13], it then rises elsewhere. Radial propagation into the SOL, seen by reflectometry [14], shows ELMs with a velocity that peaks at ~500 m/s and decays to ~120 m/s in the SOL. Probe measurements of $V_r = E_\theta B / B^2$ agree with reflectometry.

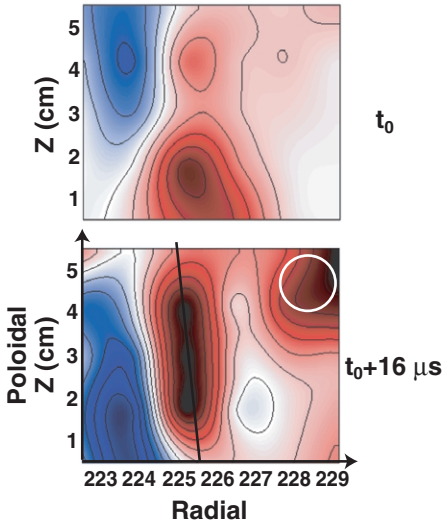

Fig. 1. Frames from BES showing 2-D density plots and taken every 1 μs. The Type I ELM starts at t_0 and a second frame is taken 16 μs thereafter is shown to illustrate ELM characteristics. The ELM shows a poloidal structure that quickly becomes quite complex. Radial and poloidal motion of ejecta is clearly seen.

The ELMs have a complex spatio-temporal structure, consistent with BES data, that is observed as multiple bursts in the temperature and density data taken by probes, shown in Fig. 2. The high time resolution data, displayed in a 12 ms window that arbitrarily spans the ELM duration. The ELM perturbation in the SOL features peak n_e values corresponding to those at the top of the density pedestal (~3×10^{19} cm^{-3}) if the spatial decay, due to parallel transport, is accounted for. Thus we suggest that the ELM peels off from the top of the density pedestal, slightly inside of the separatrix. The radial decay of

the ELM peak density and temperature with distance from the LCFS varies with density as shown in Fig. 3. At high n_e ($n_e/n_G = 0.85$) the density decay length, L_N ~ 3.8 cm while the temperature decay length, L_T is ~1.2 cm. At $n_e/n_G = 0.45$, L_N and L_T are 13 cm and 1.3 cm, respectively. At low density, the particles in the ELM travel essentially unhindered towards the wall while at high density, the particles are quickly dissipated. The heat in the ELM seems to be dissipated rapidly with radius, regardless of the pedestal density.

Probe and reflectometry data at the midplane indicate plasma being convected at ~450 m/s and slowing down to ~120 m/s into the SOL within 0.20 ms. At the highest speed, the ELM would strike the wall (6 to 7 cm from the LCFS) in ~0.15 ms, but due to the deceleration, the total radial transit time is closer to 0.3 ms for these discharges. The ***local*** peak heat and particle radial flux convected by the ELM towards the wall are $\Gamma_r = nV_r$ and Q_r = 2×3/2nTV, respectively (if $T_i = T_e$).

The ELM-induced ***local*** convected radial heat flux at the LCFS due to the bursts is ~80% of the average [calculated as ($P_{in} - P_{rad}$)/Full Area] at the LCFS, at $\langle n_e \rangle / n_{GW}$ = 0.8 and ~60% at $\langle n_e \rangle / n_{GW}$ = 0.45. However, the heat flux reaching the wall (Table I) is only a ~2% fraction of the LCFS heat flux, consistently with the short (~1.5 cm) T_e radial decay, thus most of the heat flux is transported along the magnetic field and strikes the divertor floor. The ELM local convected radial particle flux due to pulses at the wall is 10%–50% of the LCFS local average radial flux, or ~1.6×10^{21} m^{-2} s^{-1}, consistent with the long density decay length (~3 to 8 cm). Table I indicates that the ELM local peak particle flux at the wall is quite similar for all densi-

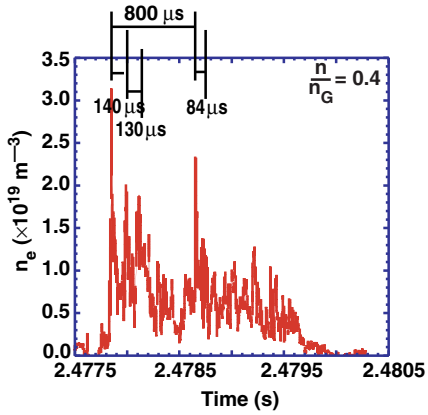

Fig. 2. High time resolution probe density data for a low discharge density (n/n_g = 0.4) showing the spatio-temporal complexity of ELMs. The successive bursts of high density lasts ~30 μs and initially appear at fairly regular intervals (~140 μs). The intervals can show some significant gaps of ~300 to 400 μs between groups of bursts.

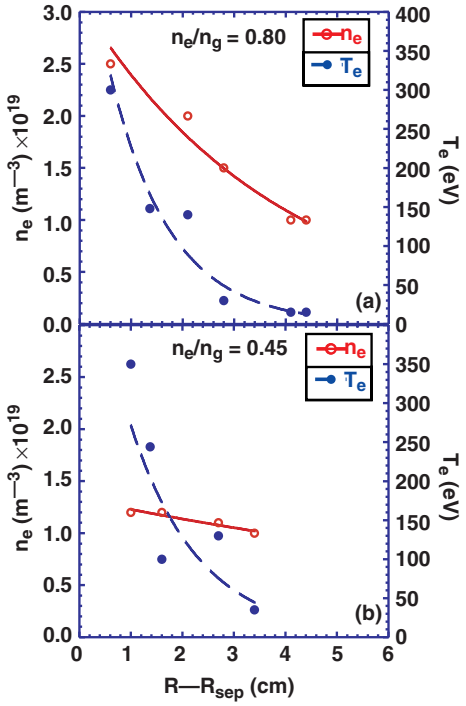

Fig. 3. Radial variation of the ELM ***burst*** density and temperature values obtained from probes for (a) high density and (b) low density discharges. The temperature decays quickly with radius in both cases, but the density decay length is much longer at low density.

ties due to the fact that at higher pedestal densities the ELM plasma density increases but the decay length becomes shorter.

Additionally, there is evidence that the ELM plasma is rotating toroidally in the SOL as seen in Fig. 4 showing CER measurements of CV emission. A transient increase in the SOL rotation appears at the start of the ELM [Fig. 4(a), vertical line], that then dampens strongly during the ELM. The values of plasma rotation and ion temperature in the LCFS during the ELM approach those at the top of the pedestal (-2 cm) before the ELM.

Table I. Radial Particle (T_r^{ELM}) and heat (Q_r^{ELM}) fluxes due to an ELM at the LCFS and the wall for low density $\langle n_e \rangle / n_{GW}$ = 0.45 high density $\langle n_e \rangle / n_{GW}$ = 0.8 discharges.

$\langle n_e \rangle / n_{GW}$=0.8	Γ_r^{ELM} ($m^{-2}s^{-1}$)	Q_r^{ELM} ($J\,m^{-2}s^{-1}$)
LCFS	1.0×10^{22}	1,800,000
Wall	1.5×10^{21}	21,600
$\langle n_e \rangle / n_{GW}$=0.45	Γ_r^{ELM} ($Jm^{-2}s^{-1}$)	Q_r^{ELM} ($J\,m^{-2}s^{-1}$)
LCFS	5.6×10^{21}	1,323,000
Wall	1.8×10^{21}	27,000

This worrk was supported by the U.S. DOE under DE-FG02-04ER54758, DE-FG03-96ER54373, DE-FC02-04ER54698, DE-FG03-01ER54615, and DE-AC04-94AL85000. Technical support of L. Chousal and R. Hernandez is acknowledged.

[1] H.D. Pacher, *et al.*, ITER Design Descrip-tion Document, ITER No. G 17 DDD 1 96-08-21 W2.1 (1996).
[2] J.W. Connor, *et al.*, Phys. Plasmas **5**, 2687 (1998).
[3] P.B. Snyder, *et al.*, Phys. Plasmas **9**, 2037 (2002).
[4] P.B. Snyder, X. Xu, private communication (2003).
[5] J.L. Luxon, Nucl. Fusion **42**, 614 (2002).
[6] D.S. Gray, *et al.*, "Time resolved radiated power during tokamak disrup-tions and spectral aver-aging of AXUV photo-diode response in DIII–D," to be published in Rev. Sci. Instrum. (2003).
[7] J.G. Watkins, *et al.*, Rev. Sci. Instrum. **63**, 4728 (1992).
[8] R.J. Fonck, *et al.*, Phys. Rev. Lett. **70**, 3736 (1993).
[9] T.L. Rhodes, *et al.*, Rev.Sci. Instrum. **63**, 4599 (1992).
[10] K.H. Burrell, Rev. Sci. Instrum. **72**, 906 (2001).
[11] D.L. Rudakov, *et al.*, Rev. Sci. Instrum. **72**, 453 (2001).
[12] L. Zeng, *et al.*, Rev. Sci. Instrum. **74**, 1530 (2003).

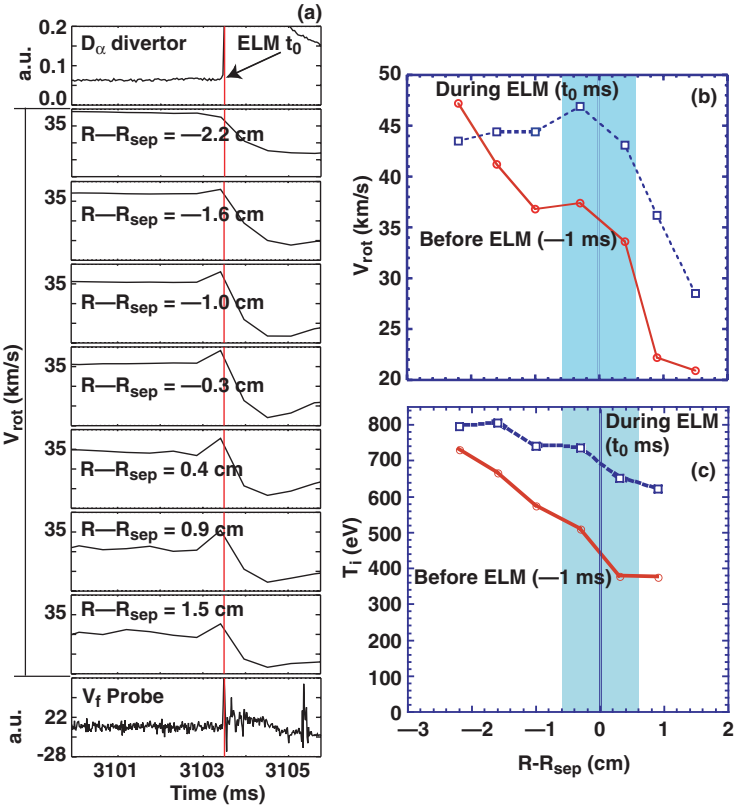

Fig. 4. (a) CER data showing the toroidal rotation velocity of carbon ions for seven radial positions inside the LCFS, and in the SOL. A floor D_α signal [(a) top] is used as a fiducial. Profiles of rotation velocity (b) and ion temperature (c) taken during the ELM (t=0) and before the ELM (t=–1) support the idea that the plasma at the top of the density pedestal is expelled into the SOL and rotates toroidally in the near SOL before being damped in the far SOL.